ELSEVIER

Trends in Food Science & Technology 18 (2007) 590–598

TRENDS IN FOOD SCIENCE & TECHNOLOGY

Review

Hyperspectral imaging – an emerging process analytical tool for food quality and safety control

A.A. Gowen[a,*], C.P. O'Donnell[a], P.J. Cullen[b], G. Downey[c] and J.M. Frias[b]

[a]Biosystems Engineering, School of Agriculture, Food Science and Veterinary Medicine, University College Dublin, Earlsfort Terrace, Dublin 2, Ireland (Tel.: +353 17165543; e-mail: aoife.gowen@ucd.ie)

[b]School of Food Science and Environmental Health, Dublin Institute of Technology, Cathal Brugha Street, Dublin 1, Ireland

[c]Teagasc Ashtown Food Research Centre, Ashtown, Dublin 15, Ireland

Hyperspectral imaging (HSI) is an emerging platform technology that integrates conventional imaging and spectroscopy to attain both spatial and spectral information from an object. Although HSI was originally developed for remote sensing, it has recently emerged as a powerful process analytical tool for non-destructive food analysis. This paper provides an introduction to hyperspectral imaging: HSI equipment, image acquisition and processing are described; current limitations and likely future applications are discussed. In addition, recent advances in the application of HSI to food safety and quality assessment are reviewed, such as contaminant detection, defect identification, constituent analysis and quality evaluation.

* Corresponding author.

0924-2244/$ - see front matter
doi:10.1016/j.tifs.2007.06.001

Introduction

Food process control necessitates real-time monitoring at critical processing points. Fast and precise analytical methods are essential to ensure product quality, safety, authenticity and compliance with labelling. Traditional methods of food monitoring involving analytical techniques such as high performance liquid chromatography (HPLC) and mass spectrometry (MS) are time consuming, expensive and require sample destruction. Near infrared spectroscopy (NIRS) is well established as a non-destructive tool for multi-constituent quality analysis of food materials (Scotter, 1990). However, the inability of NIR spectrometers to capture internal constituent gradients within food products may lead to discrepancies between predicted and measured composition. Furthermore, spectroscopic assessments with relatively small point-source measurements do not contain spatial information, which is important to many food inspection applications (Ariana, Lu, & Guyer, 2006).

Recent advances in computer technology have led to the development of imaging systems capable of identifying quality problems rapidly on the processing line, with the minimum of human intervention (Brosnan & Sun, 2004; Du & Sun, 2004). Red–Green–Blue (RGB) colour vision systems find widespread use in food quality control for the detection of surface defects and grading operations (Chao, Chen, Early, & Park, 1999; Daley, Carey, & Thompson, 1993; Throop, Aneshansley, & Upchurch, 1993). However, conventional colour cameras are poor identifiers of surface features sensitive to wavebands other than RGB, such as low but potentially harmful concentrations of animal faeces on foods (Liu, Chen, Kim, Chan, & Lefcourt, 2007; Park, Lawrence, Windham, & Smith, 2006). To overcome this, multispectral imaging systems have been developed to combine images acquired at a number (usually 3–4) of narrow wavebands, sensitive to features of interest on the object. Compared with conventional analytical methods such as HPLC, multispectral imaging systems can perform non-destructive analyses in a fraction of the time required (Malik, Poonacha, Moses, & Lodder, 2001).

Hyperspectral imaging

Hyperspectral imaging, known also as chemical or spectroscopic imaging, is an emerging technique that integrates

conventional imaging and spectroscopy to attain both spatial and spectral information from an object. It was originally developed for remote sensing applications (Goetz, Vane, Solomon, & Rock, 1985) but has since found application in such diverse fields as astronomy (Hege, O'Connell, Johnson, Basty, & Dereniak, 2003; Wood, Gulian, Fritz, & Van Vechten, 2002), agriculture (Monteiro, Minekawa, Kosugi, Akazawa, & Oda, 2007; Smail, Fritz, & Wetzel, 2006; Uno *et al*., 2005), pharmaceuticals (Lyon *et al*., 2002; Rodionova *et al*., 2005; Roggo, Edmond, Chalus, & Ulmschneider, 2005) and medicine (Ferris *et al*., 2001; Kellicut *et al*., 2004; Zheng, Chen, Intes, Chance, & Glickson, 2004). Some advantages of hyperspectral imaging over conventional RGB, NIR and multispectral imaging are outlined in Table 1.

The US Food and Drug Administration (FDA) led process analytical technology (PAT) initiative aims to understand and control the manufacturing process by monitoring critical performance attributes (http://www.fda.gov). The non-destructive, rugged and flexible nature of HSI makes it an attractive PAT for identification of critical control parameters that impact on finished product quality (Lewis, Schoppelrei, Lee, & Kidder, 2005). It is expected that HSI will be increasingly adopted as a PAT for the food industry, as has already been the case in manufacturing environments such as the pharmaceutical industry (Koehler, Lee, Kidder, & Lewis, 2002).

Hyperspectral image acquisition

Hyperspectral images are made up of hundreds of contiguous wavebands for each spatial position of a target studied. Consequently, each pixel in a hyperspectral image contains the spectrum of that specific position. The resulting spectrum acts like a fingerprint which can be used to characterise the composition of that particular pixel. Hyperspectral images, known as *hypercubes* (Lu & Chen, 1998), are three-dimensional blocks of data, comprising two spatial and one wavelength dimension, as illustrated in Fig. 1. The *hypercube* allows for the visualization of biochemical constituents of a sample, separated into particular areas of the image, since regions of a sample with similar spectral properties have similar chemical composition.

It is currently unfeasible to obtain information in all three-dimensions of a *hypercube* simultaneously; one is limited to obtaining two dimensions at a time, then creating a three-dimensional image by stacking the two-dimensional 'slices' in sequence. There are two conventional ways to construct a *hypercube*. One method, known as the "staring imager" configuration involves keeping the image field of view fixed, and obtaining images one wavelength after another. *Hypercubes* obtained using this configuration thus consist of a three-dimensional stack of images (one image for each wavelength examined), stored in what is known as the Band Sequential (BSQ) format. Wavelength in the "staring imager" configuration is typically moderated using a tuneable filter; Acousto-optic Tuneable Filters (AOTFs) and Liquid Crystal Tuneable Filters (LCTFs) are the two most predominantly employed. AOTFs have been used in the construction of commercially available NIR-CI systems (Lewis *et al*., 2005); the main advantages of AOTFs are good transmission efficiency, fast scan times and large spectral range. On the other hand, LCTFs show greater promise for filtering of Raman images, due to superior spectral bandpass and image quality (Pappas, Smith, & Winefordner, 2000). "Staring imager" instruments incorporating tuneable filters have found a number of applications in pharmaceutical quality control (Roggo *et al*., 2005; Zuzak, Schaeberle, Gladwin, Cannon, & Levin, 2001); their lack of moving parts represents an advantage in many situations.

Another configuration involves acquisition of simultaneous spectral measurements from a series of adjacent spatial positions – this requires relative movement between the object and the detector in what is known as "push-broom" acquisition (Lawrence, Park, Windham, & Mao, 2003). Some instruments produce hyperspectral images

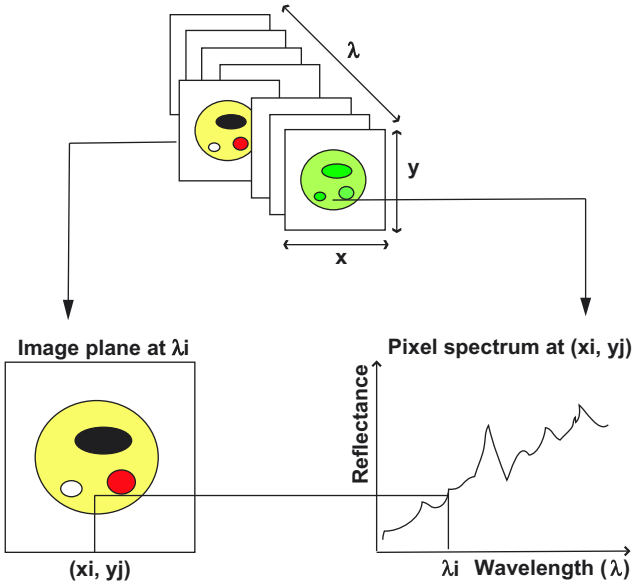

Fig. 1. Schematic representation of hyperspectral imaging *hypercube* showing the relationship between spectral and spatial dimensions.

Table 1. Comparison of RGB imaging, NIR spectroscopy (NIRS), multispectral imaging (MSI) and hyperspectral imaging (HSI)

Feature	RGB imaging	NIRS	MSI	HSI
Spatial information	✓		✓	✓
Spectral information		✓	Limited	✓
Multi-constituent information	Limited	✓	Limited	✓
Sensitivity to minor components			Limited	✓

based on a point step and acquire mode: spectra are obtained at single points on a sample, then the sample is moved and another spectrum taken. *Hypercubes* obtained using this configuration are stored in what is known as the Band Interleaved by Pixel (BIP) format. Advances in detector technology have reduced the time required to acquire *hypercubes*. Line mapping instruments record the spectrum of each pixel in a line of sample which is simultaneously recorded by an array detector; the resultant *hypercube* is stored in the Band Interleaved by Line (BIL) format. This method is particularly well suited to conveyor belt systems, and may therefore be more practicable than the former for food industry applications.

Components of a hyperspectral imaging system

Pushbroom hyperspectral imaging systems typically contain the following components: objective lens, spectrograph, camera, acquisition system, translation stage, illumination and computer, as shown in Fig. 2. The camera, spectrograph and illumination conditions determine the spectral range of the system: Vis–NIR systems typically range between 400 and 1000 nm, and utilize cameras with Charge Coupled Device (CCD) or Complementary Metal Oxide Semiconductor (CMOS) sensors; longer wavelength systems require more expensive IR focal-plane array detectors with appropriate spectrograph which operates in the IR region. The sample/target is usually diffusely illuminated by a tungsten–halogen or LED source. A line of light reflected from the sample enters the objective lens and is separated into its component wavelengths by diffraction optics contained in the spectrograph; a two-dimensional image (spatial dimension × wavelength dimension) is then formed on the camera and saved on the computer. The sample is moved past the objective lens on a motorized stage and the process repeated; two-dimensional line images acquired at adjacent points on the object are stacked to form a three-dimensional *hypercube* which may be stored on a PC for further analysis.

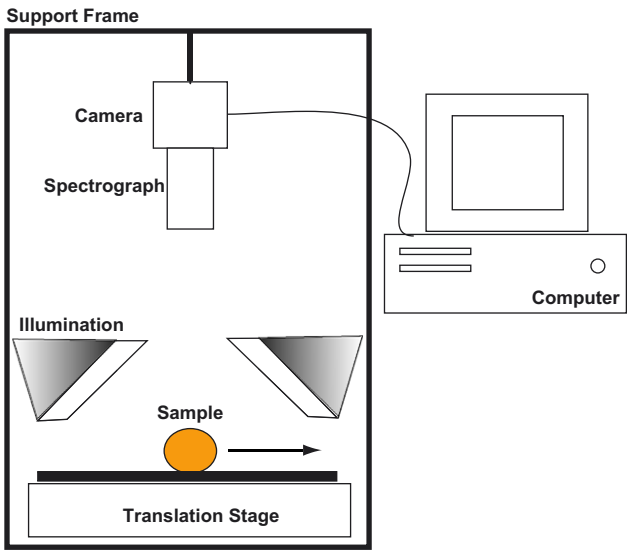

Fig. 2. Components of a hyperspectral imaging system.

Analysis of hyperspectral images

Numerous techniques exist to analyse hyperspectral data, all of which aim to reduce the dimensionality of the data while retaining important spectral information with the power to classify important areas of a scene. Typical steps followed in analysing hyperspectral images are outlined in Fig. 3 and described below.

Reflectance calibration

This is carried out to account for the background spectral response of the instrument and the 'dark' camera response. For reflectance measurements, the background is obtained by collecting a *hypercube* from a uniform, high reflectance standard or white ceramic; the dark response is acquired by turning off the light source, completely covering the lens with its cap and recording the camera response. The corrected reflectance value (R) is calculated as follows:

$$R = (\text{sample} - \text{dark})/(\text{background} - \text{dark}).$$

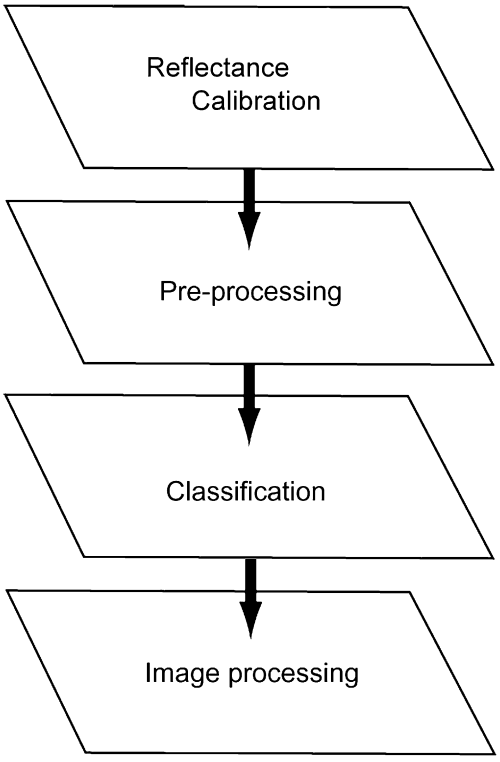

Fig. 3. Schematic diagram of hyperspectral data analysis process.

Pre-processing

Pre-processing is usually performed to remove non-chemical biases from the spectral information (e.g., scattering effects due to surface inhomogeneities) and prepare the data for further processing. A number of spectral pre-processing techniques exist, including polynomial baseline correction, Savitzky–Golay derivative conversion, mean-centering and unit variance normalisation. Other operations usually carried out at the pre-processing stage include thresholding and masking to remove redundant background information from the *hypercube*.

Classification

Hypercube classification enables the identification of regions with similar spectral characteristics. Due to the large size of *hypercubes* (which can exceed 50 MB, depending on image resolution, spectral resolution and pixel binning) complex multivariate analytical tools, such as principal component analysis (PCA), partial least squares (PLS), linear discriminant analysis (LDA), Fishers discriminant analysis (FDA), multi-linear regression (MLR) and artificial neural networks (ANN), are usually employed for classification. Table 2 presents a summary of classification algorithms utilised in 30 papers dealing with hyperspectral images of foods published since 2004 (if more than one method of analysis was used in a paper, the best performing method is shown). PLS classification was the most popular classification method, being employed in over 25% of cases.

Conventional chemometric methods such as PCA and PLS may not be suitable for analysing hyperspectral images, since these techniques were developed for analysing single spectra (Noh & Lu, 2007; Shah, Watanachaturaporn, Varshney, & Arora, 2003). To overcome this, a number of methods have been proposed: Noh and Lu (2007) applied a hybrid approach, employing both PCA and ANN to relate hyperspectral fluorescence of apple to its colour and firmness ($R > 0.75$); another research group (Cheng *et al.*, 2004) developed a hybrid PCA–FDA method for identification of chill damaged cucumbers, which outperformed PCA and FDA methods when used separately for classification. The Spectral Angle Mapper (SAM) algorithm is

Table 2. Summary of measurement mode, product type, wavelength region studied and classification algorithm employed in papers published on hyperspectral imaging of food since 2004

Mode	Product	Wavelength region (nm)	Classification	Author, year
Reflectance	Apple	447–951	Band ratio (BR)	Liu *et al.*, 2007
		430–900	Band difference (BD)	Mehl *et al.*, 2004
		954–1350	Partial least squares (PLS)	Nicolaï *et al.*, 2006
		500–950	Principal components analysis (PCA)	Xing *et al.*, 2005
		500–950	PCA	Xing, Saeys, & De Baerdemaeker, 2007
		500–950	PCA	Xing *et al.*, 2007
	Corn	950–1700	PLS	Weinstock, Janni, Hagen, & Wright, 2006
	Cucumber	900–1700	BR	Ariana *et al.*, 2006
		447–951	Integrated PCA–FDA	Cheng *et al.*, 2004
		447–951	BR	Liu *et al.*, 2005
	Citrus fruit	400–970	PLS	Menesatti, Urbani, & Lanza, 2005
	Pasta	400–1700	PLS	Menesatti D'Andrea, & Bucarelli, 2004
	Peach	500–1000	Multi-linear regression (MLR)	Lu & Peng, 2006
	Pork	430–1000	Artificial neural network (ANN)	Qiao *et al.*, 2007
	Potato	430–1000	ANN	Qiao, Wang, Ngadi, & Baljinder, 2005
	Poultry	430–850	PLS	Lawrence, Windham, Park, Heitschmidt, & Smith, 2006
		430–850	BR	Park *et al.*, 2006
		430–850	Decision tree	Windham *et al.*, 2005
		430–850	Spectral angle mapper	Park *et al.*, 2007
	Strawberry	400–1000	MLR	El Masry *et al.*, 2007
		650–1000	LDA	Tallada, Nagata, & Kobayashi, 2006
		650–1000	Band difference	Nagata, Tallada, Kobayashi, 2006
Fluorescence	Apple	500–1040	Hybrid PC-ANN	Noh & Lu, 2007
	Cantaloupe	425–774	PCA	Vargas *et al.*, 2005
	Poultry	425–710	Fuzzy algorithm	Kim *et al.*, 2004
	Walnut	425–775	Support vector machine	Jiang *et al.*, 2007
Transmittance	Cherries	450–1000	ANN	Qin & Lu, 2005
	Codfish	350–950	PLS	Heia *et al.*, 2007
	Cucumbers	450–950	Image thresholding	Ariana & Lu, 2006
	Maize	750–1090	PLS	Cogdill *et al.*, 2004

a supervised classification method which uses an *n*-dimensional angle for matching pixels to reference spectra. This method determines spectral similarity by calculating the angle between the spectra (treating them as vectors in a space with dimensionality equal to the number of wavebands), and has been used for classifying faecal and ingesta contaminants on the surface of broiler carcasses (Park, Windham, Lawrence, & Smith, 2007). Support vector machine classifiers belong to the group of machine learning algorithms that use optimization tools, which work to identify the optimal hyperplane as a decision surface to discriminate between classes of interest. A Gaussian-kernel based support vector machine approach has been used to classify walnut shell and pulp, and it was reported that this method performed better for classification than PCA and FDA (Jiang, Zhu, Rao, Berney, & Tao, 2007).

Image processing

Image processing is carried out to convert the contrast developed by the classification step into a picture depicting component distribution. Greyscale or colour mapping with intensity scaling is commonly used to display compositional contrast between pixels in an image. Image fusion, in which two or more images at different wavebands are combined to form a new image (Pohl, 1998) is frequently implemented to provide even greater contrast between distinct regions of a sample. Images may be combined using algorithms based on straightforward mathematical operators, e.g., addition, subtraction, multiplication and division. One example is the band ratio method, in which an image at one waveband is divided by that at another wavelength (Liu *et al*., 2007; Park *et al*., 2006).

Applications of hyperspectral imaging to food quality and safety

Hyperspectral imaging is a powerful tool for the identification of key wavebands in the development of online automated multispectral imaging systems. Consequently, it finds widespread use in research for the development of multispectral inspection tools. Hyperspectral imaging, like other spectroscopy techniques, can be carried out in reflectance, transmission or fluorescence modes. While the majority of published research on hyperspectral imaging has been performed in reflectance mode, transmission and emission modes have also been investigated: the following contains descriptions of the recent advances in the application of hyperspectral imaging in each of these modes for food quality analysis.

Hyperspectral reflectance imaging

Reflectance is the most common mode of hyperspectral imaging, with 22 out of 30 research papers published since 2004 performed in reflectance mode (Table 2). Hyperspectral reflectance imaging is usually carried out in the Vis–NIR (400–1000 nm) or NIR (1000–1700 nm) range, and has been used to detect defects, contaminants and quality attributes of fruits, vegetables and meat products, as described below.

One research team (Nicolaï, Lötze, Peirs, Scheerlinck, & Theron, 2006) developed an NIR hyperspectral reflectance system with a spectral range of 900–1700 nm to detect the bitter pit defect in apples. The system was capable of identifying bitter pit lesions invisible to the naked eye, but reduced luminosity at the image boundary caused some misclassification errors. Ariana *et al*. (2006) investigated the application of NIR hyperspectral reflectance imaging in the same spectral region for the detection of bruises on pickling cucumbers. Reflectance for bruised cucumber tissue was generally lower than that for normal tissue, and detection accuracy was dependent on the time after bruising. It was demonstrated that band ratio and difference algorithms were better than PCA for classification of bruised cucumbers.

Light scattering from a surface is highly dependent on the product density and cell structures, so it follows that scattering profiles may indicate related properties, such as texture. Indeed, the relationship between hyperspectral scattering profiles (in the 500–1000 nm spectral range) and texture has been explored to predict peach firmness (Lu & Peng, 2006). In this investigation, a Lorentzian distribution function was fitted to scattering data, and Lorentzian model parameters at each wavelength were used to build an empirical regression model to predict peach firmness ($R > 0.58$).

A Vis–NIR (400–1000 nm) hyperspectral reflectance imaging system was developed to identify bruises on apples (Xing, Bravo, Jancsók, Ramon, & De Baerdemaeker, 2005). Using PCA, four wavebands were selected to build a multispectral testing system; PCA was then applied to the multispectral images, and it was shown that the 2nd and 3rd principal components could identify bruises with 86% accuracy. Xing, Saeys, and De Baerdemaeker (2006) also developed a multispectral imaging system to discriminate between bruises and the stem-end/calyx on apples, a well known problem in apple sorting technology. Polder, Heijden, and Young (2002) showed that a hyperspectral reflectance imaging system in the spectral region of 396–736 nm was more effective than RGB imaging for discriminating ripeness level in tomatoes, regardless of illumination condition tested. El Masry, Wang, El Sayed, and Ngadi (2007) used a Vis–NIR hyperspectral imaging system region for non-destructive determination of strawberry quality. Optimal wavelengths were obtained from PLS, and multi-linear regression was then used to predict moisture content, total soluble solids content and pH ($R > 0.8$). A similar system was used to evaluate pork quality and marbling level (Qiao, Ngadi, Wang, Gariépy, & Prasher, 2007), employing a feed-forward neural network to classify samples, with up to 85% classification accuracy.

Gómez-Sanchis *et al.* (2004) demonstrated the potential of using a Vis–NIR hyperspectral imaging system for the detection of infections caused by *Penicillium digitatum* in citrus fruits before they became apparent to human inspectors. PCA was employed to reduce the number of detection wavebands, and classification and regression trees were applied which correctly classified 80% of image pixels. Park *et al.* (2006) investigated the performance of a Vis–NIR hyperspectral reflectance imaging system for poultry surface faecal contaminant detection. The system allowed for the selection of optimum bandwidths for the construction of a multispectral imaging system based on dual band ratio algorithm to identify ingesta and faeces on poultry carcasses with 96.4% accuracy.

The research group of Kim, Chen, and Mehl (2001) developed a laboratory-based hyperspectral imaging system with a spectral range of 430–930 nm to conduct food quality and safety research, primarily for the development of multispectral imaging systems for food process control, through detection of optimal bands and algorithm development. This system was recently used to conduct hyperspectral reflectance imaging experiments for the detection of apple surface defects/contamination (Kim *et al.*, 2002; Liu *et al.*, 2007; Mehl, Chen, Kim, & Chan, 2004) and identification of chilling damage on cucumber (Cheng *et al.*, 2004; Liu, Chen, Wang, Chan, & Kim, 2005). Both Kim *et al.* (2002) and Liu *et al.* (2007) have stated that hyperspectral reflectance imaging was unable to detect thin layers of faeces on apples, and suggested that use of fluorescence hyperspectral imaging would improve detection rates, noting, however, the relatively high cost of laser excitation sources.

Hyperspectral fluorescence imaging

Fluorescence spectroscopy is well established as an analytical technique for food control, especially in the dairy industry (Christensen, Povlsen, & Sørensen, 2003; Karoui & De Baerdemaeker, 2007; Strasburg & Lude, 1995). The chlorophyll chromophore is particularly important for the fluorescence of plant products, and plants excited by UV light generally emit in the visible–near infrared region (Chappelle, McMurtrey, & Kim, 1991). Hyperspectral fluorescence imaging is emerging as a tool for food quality investigation: 4 out of 30 papers published on hyperspectral imaging applied to food since 2004 have investigated hyperspectral fluorescence imaging (Table 2).

Kim, Kim, Chen, and Kong (2004) designed a hyperspectral fluorescence system to detect skin tumours on chicken carcasses. UV-A (365 nm) lamps were used to illuminate samples on a moving stage and hyperspectral images were obtained by acquiring adjacent line scans, as described previously. A multispectral imaging system was developed by the same research group to detect faecal contamination on apples, based on optimal wavelengths identified by a hyperspectral fluorescence imaging system (Kim *et al.*, 2002). This research team also used hyperspectral fluorescence images to develop a multispectral system for detection of faecal contamination on pork and apple, using a 355 nm Nd:Yag laser for excitation (Kim, Lefcourt, & Chen, 2003). Regions of contamination not readily visible to the human eye were easily identified from the multispectral fluorescence images obtained. Vargas, Kim, Tao, and Lefcourt (2005) investigated hyperspectral fluorescence imaging for the detection of faecal contamination on cantaloupes, employing PCA to identify dominant wavelengths for the development of a multispectral detection system.

Noh and Lu (2007) examined the relationship between fluorescence hyperspectral line images and apple quality, using a blue-laser diode to produce chlorophyll fluorescence: a hyperspectral line scan located 1.5 mm from the beam centre was analysed using a hybrid PCA–ANN method. No significant differences were observed from fluorescence data obtained after 1, 2, 3, 4 and 5 min of continuous laser illumination; therefore, fluorescence measurements could be performed within 1 min of illumination. Spectral features were correlated to apple quality characteristics such as firmness and colour with a correlation coefficient of 0.74 or greater after 1 min illumination. It was noted that the relatively low correlation coefficients obtained in the study could be improved by using multiple line scans rather than single line scans.

Hyperspectral transmission imaging

Only 4 out of 30 papers published on hyperspectral imaging of food since 2004 have dealt with hyperspectral imaging in the transmission mode (Table 2). Transmission hyperspectral imaging is potentially applicable for the online estimation of internal constituent concentrations and detection of internal defects within foods (Schmilovitch *et al.*, 2004). Qin and Lu (2005) applied hyperspectral transmission imaging to detect pits in tart cherries. Light was transmitted through individual cherries from a light source placed below the sample holder, and recorded by an imaging spectrograph placed above the sample. Transmission images for four different sample orientations were tested, and it was shown that sample orientation and colour did not significantly affect classification accuracy. This is significant for high throughput operations, where it is difficult to keep sample orientation uniform. Cogdill, Hurburgh, and Rippke (2004) investigated the application of NIR hyperspectral transmission imaging for estimation of oil and moisture content in corn kernels. Stationary samples were illuminated from below *via* collimating optics through a sample presentation stage: a tuneable filter within the spectrograph removed the need for sample movement. Although this method was capable of predicting moisture content with high accuracy, it was unable to measure oil concentration

accurately. Another research team (Heia *et al*., 2007) developed a detection method for parasites on codfish, by applying PLS regression to transmission hyperspectral images. This method enabled non-destructive identification of parasites 2–3 mm deeper than could be detected by manual inspection of fillets.

Transmission hyperspectral images may equally be obtained from moving samples. Ariana and Lu (2006) employed such an approach to investigate internal damage in cucumbers. Cucumbers were mounted on a rotating stage, illuminated from below and hyperspectral transmission line scans were captured from above. Three hyperspectral line scans were obtained for each cucumber, separated by 120°. An image thresholding method resulted in higher classification accuracies than PLS analysis, achieving overall classification accuracy up to 94.3%.

Hyperspectral imaging for bacterial identification

Recently, a number of researchers have reported the potential of HSI for identification of microorganisms of concern in food. Dubois, Lewis, Fry, and Calvey (2005) demonstrated the potential application of NIR hyperspectral imaging as a high throughput technique for the differentiation of bacteria based on their NIR spectra. NIR images of food specific cards containing both test and calibration bacteria samples were obtained in the spectral region 1200–2350 nm using an InSb focal-plane array detector. Some bacteria were identifiable from spectral differences observed at unique wavelengths; however, in situations where particular microorganisms of concern were sought, PLS classification was preferable to separate the genera of bacteria present. The suitability of Raman hyperspectral imaging for the enumeration of waterborne pathogens has also been evaluated (Escoriza, VanBriesen, Stewart, Maier, & Treado, 2006). Hyperspectral images in the range 3200–3700 nm were obtained from inoculated water samples using a Raman Chemical Imaging microscope containing a liquid crystal tuneable filter. It was shown that Raman hyperspectral imaging can provide quantitative information for bacterial concentration in water samples. It was noted, however, that the Raman signal was poor for low bacteria concentration ($\leq 1 \times 10^7$ cells/membrane), necessitating the use of filters on dilute water samples prior to examination.

Limitations

HSI is a powerful platform technology for food process monitoring. Currently, however, there are two major barriers to its widespread adoption in the food industry. The first is the high purchase cost of HSI systems: since this technology is emerging as a tool for food quality evaluation, there are few commercial suppliers. It is anticipated that future technological developments in HSI systems for the pharmaceutical industry will promote the manufacture of low cost systems suitable for food industry applications. The second limiting factor arises from the relatively lengthy times necessary for *hypercube* image acquisition, processing and classification (Chen, Chao, & Kim, 2002), depending on target size and image resolution, acquisition time can range from 2 to 4 min, while processing and classification time are largely dependent on computer hardware and software capabilities. However, it can be expected that future developments in system components, such as improved cameras, faster hardware, more accurate and efficient algorithms, will shorten processing and acquisition time, enabling real-time HSI quality monitoring systems.

Conclusions

Hyperspectral imaging (HSI) is an emerging tool for food quality and safety analysis; the spatial feature of HSI enables characterisation of complex heterogeneous samples, while the spectral feature allows for the identification of a wide range of multi-constituent surface and sub-surface features. Due to the current high cost of HSI systems, most food related HSI research has been geared towards identification of important wavebands for the development of low cost multispectral imaging systems. However, judging by the continuing emphasis on process analytical technologies to provide accurate, rapid, non-destructive analysis of foodstuffs, it is likely that hyperspectral imaging will be increasingly adopted for safety and quality control in the food industry, as has already been the case in the pharmaceutical industry. Future developments in HSI equipment manufacture, such as lower purchase costs and improvements in processing speed, will encourage more widespread utilisation of this emerging platform technology.

Acknowledgement

The authors would like to acknowledge the funding of the Irish Government Department of Agriculture and Food under the Food Institutional Research Measure (FIRM).

References

Ariana, D., & Lu, R. (2006). Visible/near-infrared hyperspectral transmittance imaging for detection of internal mechanical injury in pickling cucumbers. In: *ASABE Annual International Meeting,* Paper No. 063039, July 2006.

Ariana, D., Lu, R., & Guyer, D. E. (2006). Hyperspectral reflectance imaging for detection of bruises on pickling cucumbers. *Computers and Electronics in Agriculture, 53*(1), 60–70.

Brosnan, T., & Sun, D. W. (2004). Improving quality inspection of food products by computer vision – a review. *Journal of Food Engineering, 61*, 3–16.

Chao, K., Chen, Y. R., Early, H., & Park, B. (1999). Color image classification systems for poultry viscera inspection. *Applied Engineering in Agriculture, 15*(4), 363–369.

Chappelle, E., McMurtrey, J., & Kim, M. S. (1991). Identification of the pigment responsible for the blue fluorescence band in the laser induced fluorescence (LIF) spectra of green plants, and the

potential use of this band in remotely estimating rates of photosynthesis. *Remote Sensing of Environment*, *36*(3), 213–218.
Chen, Y. R., Chao, K., & Kim, M. S. (2002). Machine vision technology for agricultural applications. *Computers and Electronics in Agriculture*, *36*(2), 173–191.
Cheng, X., Chen, Y. R., Tao, Y., Wang, C. Y., Kim, M. S., & Lefcourt, A. M. (2004). A novel integrated PCA and FLD method on hyperspectral image feature extraction for cucumber chilling damage inspection. *Transactions of ASAE*, *47*(4), 1313–1320.
Christensen, J., Povlsen, V. T., & Sørensen, J. (2003). Application of fluorescence spectroscopy and chemometrics in the evaluation of processed cheese during storage. *Journal of Dairy Science*, *86*, 1101–1107.
Cogdill, R., Hurburgh, C., & Rippke, G. (2004). Single-kernel maize analysis by near-infrared hyperspectral imaging. *Transactions of the ASAE*, *47*(1), 311–320.
Daley, W., Carey, R., & Thompson, C. (1993). Poultry grading/inspection using color imaging. *Proceedings of the SPIE*, *1907*, 124–132.
Du, C. J., & Sun, D. W. (2004). Recent developments in the applications of image processing techniques for food quality evaluations. *Trends in Food Science & Technology*, *15*, 230–249.
Dubois, J., Lewis, E., Fry, F., & Calvey, E. (2005). Bacterial identification by near-infrared chemical imaging of food-specific cards. *Food Microbiology*, *22*(6), 577–583.
El Masry, G., Wang, N., El Sayed, A., & Ngadi, M. (2007). Hyperspectral imaging for nondestructive determination of some quality attributes for strawberry. *Journal of Food Engineering*, *81*(1), 98–107.
Escoriza, M., VanBriesen, J., Stewart, S., Maier, J., & Treado, P. (2006). Raman spectroscopy and chemical imaging for quantification of filtered waterborne bacteria. *Journal of Microbiological Methods*, *66*(1), 63–72.
Ferris, D., Lawhead, R., Dickman, E., Holtzapple, N., Miller, J., Grogan, S., et al. (2001). Multimodal hyperspectral imaging for the noninvasive diagnosis of cervical neoplasia. *Journal of Lower Genital Tract Disease*, *5*(2), 65–72.
Goetz, A. F. H., Vane, G., Solomon, T. E., & Rock, B. N. (1985). Imaging spectrometry for earth remote sensing. *Science*, *228*, 1147–1153.
Gómez-Sanchis, J., Moltó, E., Gomez-Chova, L., Aleixos, N., Camps-Valls, G., Juste, F., et al. (2004). Hyperspectral computer vision system for the detection of *Penicillium digitatum* in citrus packing lines. In: *2004 CIGR International Conference*, Beijing, China, 11–14 October 2004.
Hege, E., O'Connell, D., Johnson, W., Basty, S., & Dereniak, E. (2003). Hyperspectral imaging for astronomy and space surveillance. *Proceedings of the SPIE*, *5159*, 380–391.
Heia, K., Sivertsen, A., Stormo, S., Elvevoll, E., Wold, J., & Nilsen, H. (2007). Detection of nematodes in Cod (*Gadus morhua*) fillets by imaging spectroscopy. *Journal of Food Science*, *72*(1), E011–E015.
Jiang, L., Zhu, B., Rao, X., Berney, G., & Tao, Y. (2007). Discrimination of black walnut shell and pulp in hyperspectral fluorescence imagery using Gaussian kernel function approach. *Journal of Food Engineering*, *81*(1), 108–117.
Karoui, R., & De Baerdemaeker, J. (2007). A review of the analytical methods coupled with chemometric tools for the determination of the quality and identity of dairy products. *Food Chemistry*, *102*(3), 621–640.
Kellicut, D., Weiswasser, J., Arora, S., Freeman, J., Lew, R., Shuman, C., et al. (2004). Emerging technology: hyperspectral imaging. *Perspectives in Vascular Surgery and Endovascular Therapy*, *16*(1), 53–57.
Kim, I., Kim, M. S., Chen, Y. R., & Kong, S. G. (2004). Detection of skin tumors on chicken carcasses using hyperspectral fluorescence imaging. *Transactions of the ASAE*, *47*(5), 1785–1792.
Kim, M. S., Chen, Y. R., & Mehl, P. M. (2001). Hyperspectral reflectance and fluorescence imaging system for food quality and safety. *Transactions of the ASAE*, *44*(3), 721–729.
Kim, M. S., Lefcourt, A. M., Chao, K., Chen, Y. R., Kim, I., & Chan, D. E. (2002). Multispectral detection of fecal contamination on apples based on hyperspectral imagery: Part I. Application of visible and near-infrared reflectance imaging. *Transactions of the ASAE*, *45*(6), 2027–2037.
Kim, M. S., Lefcourt, A. M., & Chen, Y. R. (2003). Multispectral laser-induced fluorescence imaging system for large biological samples. *Applied Optics*, *42*(19), 3927–3933.
Koehler, F., Lee, E., Kidder, L., & Lewis, N. (2002). Near infrared spectroscopy: the practical chemical imaging solution. *Spectroscopy Europe*, *14*(3), 12–19.
Lawrence, K. C., Park, B., Windham, W. R., & Mao, C. (2003). Calibration of a pushbroom hyperspectral imaging system for agricultural inspection. *Transactions of the ASAE*, *46*(2), 513–521.
Lawrence, K. C., Windham, W. R., Park, B., Heitschmidt, G. W., Smith, D. P., & Feldner, P. (2006). Partial least squares regression of hyperspectral images for contaminant detection on poultry carcasses. *Journal of Near Infrared Spectroscopy*, *14*(4), 223–230.
Lewis, E., Schoppelrei, J., Lee, E., & Kidder, L. (2005). Near-infrared chemical imaging as a process analytical tool. In: K. Bakeev (Ed.), *Process analytical technology* (pp. 187). Oxford: Blackwell Publishing.
Liu, Y., Chen, Y. R., Kim, M. S., Chan, D. E., & Lefcourt, A. M. (2007). Development of simple algorithms for the detection of fecal contaminants on apples from visible/near infrared hyperspectral reflectance imaging. *Journal of Food Engineering*, *81*(2), 412–418.
Liu, Y., Chen, Y. R., Wang, C. Y., Chan, D. E., & Kim, M. S. (2005). Development of simple algorithm for the detection of chilling injury in cucumbers from visible/near-infrared hyperspectral imaging. *Applied Spectroscopy*, *59*(1), 78–85.
Lu, R. F., Chen, Y. R. (1998). Hyperspectral imaging for safety inspection of food and agricultural products. In: *SPIE Conference on Pathogen Detection and Remediation for Safe Eating*, Boston, November 1998.
Lu, R. F., & Peng, Y. K. (2006). Hyperspectral scattering for assessing peach fruit firmness. *Biosystems Engineering*, *93*(2), 161–171.
Lyon, R. C., Lester, D. S., Lewis, E. N., Lee, E., Yu, L. X., Jefferson, E. H., et al. (2002). Near-infrared spectral imaging for quality assurance of pharmaceutical products: analysis of tablets to assess powder blend homogeneity. *AAPS PharmSciTech*, *3*(3), 17.
Malik, I., Poonacha, M., Moses, J., & Lodder, R. A. (2001). Multispectral imaging of tablets in blister packaging. *AAPS PharmSciTech*, *2*(2), 9.
Mehl, P. M., Chen, Y. R., Kim, M. S., & Chan, D. E. (2004). Development of hyperspectral imaging technique for the detection of apple surface defects and contaminations. *Journal of Food Engineering*, *61*(1), 67–81.
Menesatti, P., D'Andrea, & S., Bucarelli, A. (2004). Non-destructive spectrometric qualification of Italian wheat durum pasta produced by traditional or industrial technology approaches. In: *2004 CIGR International Conference*, Beijing, China, 11–14 October 2004.
Menesatti, P., Urbani, G., & Lanza, G. (2005). Spectral imaging Vis–NIR system to forecast the chilling injury onset on citrus fruits. In: F. Mencarelli, & P. Tonutti (Eds.), *ISHS Acta Horticulturae 682: V International Postharvest Symposium* (pp. 1347–1354). ISHS.
Monteiro, S., Minekawa, Y., Kosugi, Y., Akazawa, T., & Oda, K. (2007). Prediction of sweetness and amino acid content in soybean crops from hyperspectral imagery. *ISPRS Journal of Photogrammetry and Remote Sensing*, *62*(1), 2–12.

Nagata, M., Tallada, J., & Kobayashi, T. (2006). Bruise detection using NIR hyperspectral imaging for strawberry (*Fragaria* × *ananassa* Duch.). *Environment Control in Biology*, *44*(2), 133–142.

Nicolaï, B., Lötze, E., Peirs, A., Scheerlinck, N., & Theron, K. (2006). Non-destructive measurement of bitter pit in apple fruit using NIR hyperspectral imaging. *Postharvest Biology and Technology*, *40*, 1–6.

Noh, H., & Lu, R. (2007). Hyperspectral laser-induced fluorescence imaging for assessing apple fruit quality. *Postharvest Biology and Technology*, *43*, 193–201.

Pappas, D., Smith, B. W., & Winefordner, J. D. (2000). Raman imaging for two-dimensional chemical analysis. *Applied Spectroscopy Reviews*, *35*, 1–23.

Park, B., Lawrence, K. C., Windham, W. R., & Smith, D. (2006). Performance of hyperspectral imaging system for poultry surface fecal contaminant detection. *Journal of Food Engineering*, *75*(3), 340–348.

Park, B., Windham, W. R., Lawrence, K. C., & Smith, D. (2007). Contaminant classification of poultry hyperspectral imagery using a spectral angle mapper algorithm. *Biosystems Engineering*, *96*(3), 323–333.

Pohl, C. (1998). Multisensor image fusion in remote sensing. *International Journal of Remote Sensing*, *19*(5), 823–854.

Polder, G., Heijden, G., & Young, I. (2002). Spectral image analysis for measuring ripeness of tomatoes. *Transactions of the ASAE*, *45*, 1155–1161.

Qiao, J., Ngadi, M., Wang, N., Gariépy, C., & Prasher, S. (2007). Pork quality and marbling level assessment using a hyperspectral imaging system. *Journal of Food Engineering*, *83*(1), 10–16.

Qiao, J., Wang, N., Ngadi, M., & Baljinder, S. (2005). *Water content and weight estimation for potatoes using hyperspectral imaging*. St. Joseph, Michigan: The American Society of Agricultural and Biological Engineers. www.asabe.org. Paper number 053126, 2005 ASAE Annual Meeting.

Qin, J., & Lu, R. (2005). Detection of pits in tart cherries by hyperspectral transmission imaging. *Transactions of the ASAE*, *48*(5), 1963–1970.

Rodionova, O., Houmøller, L., Pomerantsev, A., Geladi, P., Burger, J., Dorofeyev, V., et al. (2005). NIR spectrometry for counterfeit drug detection: a feasibility study. *Analytica Chimica Acta*, *549*(1–2), 151–158.

Roggo, Y., Edmond, A., Chalus, P., & Ulmschneider, M. (2005). Infrared hyperspectral imaging for qualitative analysis of pharmaceutical solid forms. *Analytica Chimica Acta*, *535*(1–2), 79–87.

Schmilovitch, Z., Shenderey, C., Shmulevich, I., Alchanatis, V., Egozi, H., Hoffman, A., et al. (2004). NIRS detection of mouldy core in apples. In: *2004 CIGR International Conference*, Beijing, China, 11–14 October 2004.

Scotter, C. (1990). Use of near infrared spectroscopy in the food industry with particular reference to its applications to on/in-line food processes. *Food Control*, *1*(3), 142–149.

Shah, C. A., Watanachaturaporn, P., Varshney, P. K., & Arora, M. K. (2003). Some recent results on hyperspectral image classification. In: *Proceedings of IEEE Workshop on Advances in Techniques for Analysis of Remotely Sensed Data* (pp. 346–353). Greenbelt, MD, 27–28 October 2003.

Smail, V., Fritz, A., & Wetzel, D. (2006). Chemical imaging of intact seeds with NIR focal plane array assists plant breeding. *Vibrational Spectroscopy*, *42*(2), 215–221.

Strasburg, G., & Lude, R. (1995). Theory and applications of fluorescence spectroscopy in food research. *Trends in Food Science & Technology*, *6*(3), 69–75.

Tallada, J., Nagata, M., & Kobayashi, T. (2006). Non-destructive estimation of firmness of strawberries (*Fragaria* × *ananassa* Duch.) using NIR hyperspectral imaging. *Environment Control in Biology*, *44*(4), 245–255.

Throop, J. A., Aneshansley, D. J., & Upchurch, B. L. (1993). Near-IR and color imaging for bruise detection on Golden Delicious apples. *Proceedings of SPIE*, *1836*, 33–44.

Uno, Y., Prasher, S., Lacroix, R., Goel, P., Karimi, Y., Viau, A., et al. (2005). Artificial neural networks to predict corn yield from Compact Airborne Spectrographic Imager data. *Computers and Electronics in Agriculture*, *47*(2), 149–161.

Vargas, A. M., Kim, M. S., Tao, Y., & Lefcourt, A. (2005). Detection of fecal contamination on cantaloupes using hyperspectral fluorescence imagery. *Journal of Food Science*, *70*(8), E471–E476.

Weinstock, B. A., Janni, J., Hagen, L., & Wright, S. (2006). Prediction of oil and oleic acid concentrations in individual corn (*Zea mays* L.) kernels using near-infrared reflectance hyperspectral imaging and multivariate analysis. *Applied Spectroscopy*, *60*(1), 9–16.

Wood, K. S., Gulian, A. M., Fritz, G. G., & Van Vechten, D. (2002). A QVD detector for focal plane hyperspectral imaging in astronomy. *Bulletin of the American Astronomical Society*, *34*, 1241.

Xing, J., Bravo, C., Jancsók, P., Ramon, H., & De Baerdemaeker, J. (2005). Detecting bruises on 'Golden Delicious' apples using hyperspectral imaging with multiple wavebands. *Biosystems Engineering*, *90*(1), 27–36.

Xing, J., Jancsók, P., & De Baerdemaeker, J. (2006). Stem-end/calyx identification on apples using contour analysis in multispectral images. *Biosystems Engineering*, *96*(2), 231–237.

Xing, J., Saeys, W., & De Baerdemaeker, J. (2007). Combination of chemometric tools and image processing for bruise detection on apples. *Computers and Electronics in Agriculture*, *56*(1), 1–13.

Zheng, G., Chen, Y., Intes, X., Chance, B., & Glickson, J. D. (2004). Contrast-enhanced near-infrared (NIR) optical imaging for subsurface cancer detection. *Journal of Porphyrins and Phthalocyanines*, *8*(9), 1106–1117.

Zuzak, K., Schaeberle, M., Gladwin, M., Cannon, R., & Levin, I. (2001). Noninvasive determination of spatially resolved and time-resolved tissue perfusion in humans during nitric oxide inhibition and inhalation by use of a visible-reflectance hyperspectral imaging technique. *Circulation*, *104*, 2905.